Proc. Natl. Acad. Sci. USA
Vol. 93, pp. 407–411, January 1996
Medical Sciences

Targeted disruption of gp130, a common signal transducer for the interleukin 6 family of cytokines, leads to myocardial and hematological disorders

(myocardial development/hematopoiesis)

KANJI YOSHIDA*, TETSUYA TAGA*, MIKIYOSHI SAITO*, SACHIKO SUEMATSU†, ATSUSHI KUMANOGOH*, TAKASHI TANAKA*†‡, HIROSHI FUJIWARA†‡, MORITOSHI HIRATA‡, TAMOTSU YAMAGAMI‡, TATSUTOSHI NAKAHATA§, TOMOKO HIRABAYASHI¶, YOSHIHIRO YONEDA¶, KAZUHIKO TANAKA‖, WEI-ZHONG WANG**, CHISATO MORI**, KOHEI SHIOTA**, NOBUAKI YOSHIDA†, AND TADAMITSU KISHIMOTO‡

*Institute for Molecular and Cellular Biology, Osaka University, Osaka 565, Japan; †Department of Immunology, Research Institute, Osaka Medical Center for Maternal and Child Health, Osaka 590-02, Japan; ‡Department of Medicine III, Osaka University Medical School, Osaka 565, Japan; §Department of Clinical Oncology, The Institute of Medical Science, The University of Tokyo, Tokyo 108, Japan; ¶Department of Anatomy and Cell Biology, Osaka University Medical School, Osaka 565, Japan; ‖Department of Structural Biology, Research Institute, The Center for Adult Disease, Osaka, Osaka 537, Japan; and **Department of Anatomy and Developmental Biology, Kyoto University Faculty of Medicine, Kyoto 606, Japan

Contributed by Tadamitsu Kishimoto, October 5, 1995

ABSTRACT **gp130 is a ubiquitously expressed signal-transducing receptor component shared by interleukin 6, interleukin 11, leukemia inhibitory factor, oncostatin M, ciliary neurotrophic factor, and cardiotrophin 1. To investigate physiological roles of gp130 and to examine pathological consequences of a lack of gp130, mice deficient for gp130 have been prepared. Embryos homozygous for the gp130 mutation progressively die between 12.5 days postcoitum and term. On 16.5 days postcoitum and later, they show hypoplastic ventricular myocardium without septal and trabecular defect. The subcellular ultrastructures in gp130$^{-/-}$ cardiomyocytes appear normal. The mutant embryos have greatly reduced numbers of pluripotential and committed hematopoietic progenitors in the liver and differentiated lineages such as T cells in the thymus. Some gp130$^{-/-}$ embryos show anemia due to impaired development of erythroid lineage cells. These results indicate that gp130 plays a crucial role in myocardial development and hematopoiesis during embryogenesis.**

Cytokine signals are mediated through specific receptor complexes, whose components belong, in most cases, to a large group of proteins called the cytokine receptor family (1). These receptor complexes are usually composed of a ligand-specific receptor chain and a signal transducer common to multiple cytokines. gp130 was initially identified as a signal transducing receptor component that associates with the interleukin 6 receptor (IL-6R) when the receptor binds interleukin 6 (IL-6) (2). gp130 is also utilized as a critical signaling component in the receptor complexes for interleukin 11, leukemia inhibitory factor (LIF), oncostatin M, ciliary neurotrophic factor (CNTF), and cardiotrophin 1 (CT-1) (refs. 1 and 3 and references therein). The discovery of this shared signal transducer, gp130, helps to explain how these different cytokines mediate overlapping biological functions. IL-6 binding to IL-6R induces homodimerization of gp130 (4), whereas stimulation by LIF, CNTF, oncostatin M, and CT-1 leads to heterodimerization of gp130 with a closely related protein, LIF receptor (3, 5). Homo- or heterodimerization of gp130 triggers the activation of JAK1, JAK2, and TYK2, members of the JAK family of cytoplasmic tyrosine kinases that are associated with gp130 (6–8). This leads to subsequent tyrosine phosphorylation and functional activation of a latent cytoplasmic transcription factor, APRF/STAT3 (for acute phase response factor or signal transducer and activator of transcription 3) (8–10), and the Ras/MAPK (mitogen-activated protein kinase) cascade (11).

gp130 is ubiquitously expressed in almost all organs, including heart, spleen, kidney, lung, liver, placenta, and brain (12). In contrast, expression of the ligand-binding receptor chains shows somewhat restricted distribution and does not necessarily parallel that of gp130. From the developmental point of view, gp130 is expressed at relatively high levels in embryos and placentas. Its expression is observed even in embryonic stem (ES) cells (12). The normal physiological role of gp130 expressed in this broad range of tissues has not fully been elucidated. In addition, no disease has so far been identified for which an abnormality in the gp130-signaling pathway is responsible. In this regard, mice lacking IL-6, LIF, or CNTF have been generated, but they manifest phenotypes that are much less severe than would be expected from the known pleiotropic functions of these cytokines (13–15). This is probably because their functions can be compensated for by other gp130-stimulatory cytokines. To examine physiological roles of gp130 and to understand pathological consequences resulting from the lack of this common signal transducer, we have created mice deficient for gp130.

MATERIALS AND METHODS

Gene Targeting. Genomic clones for the mouse gp130 gene were obtained by screening a BALB/c liver library with a mouse gp130 cDNA probe (ref. 12, K.Y., unpublished data). A pMC1Neo-poly(A) cassette was inserted into the *Hin*dIII site in exon 2 just downstream of the translational initiation codon to facilitate positive selection of integration events, and the MC1 herpes simplex virus thymidine kinase gene was added to the 5′ end for negative selection of nonhomologous recombination (ref. 16; see Fig. 1). E14.1 ES cells were transfected with the *Bam*HI-linearized gp130 targeting vector (20 μg for 10^7 cells) by electroporation and cultured on irradiated STO feeder cells. G418 (400 μg/ml, GIBCO) and gancyclovir (2 μM, provided by Syntex, Ibaraki Japan) were added 1 and 6 days later, respectively. After 6 more days, resistant colonies were picked and genomic DNA was analyzed for homologous

The publication costs of this article were defrayed in part by page charge payment. This article must therefore be hereby marked "*advertisement*" in accordance with 18 U.S.C. §1734 solely to indicate this fact.

Abbreviations: IL-6, interleukin 6; LIF, leukemia inhibitory factor; CNTF, ciliary neurotrophic factor; CT-1, cardiotrophin 1; dpc, days postcoitum; IL-6R, IL-6 receptor; sIL-6R, soluble IL-6R; ES, embryonic stem; CFU-S, colony-forming units in spleen; MNC, mononuclear cells; BFU-E, erythroid burst-forming units; CFU-GM, granulocyte/macrophage colony-forming units.

recombination by PCR, which was subsequently confirmed by Southern blot analysis.

Histological Analysis. Embryos fixed in phosphate-buffered saline containing 3.7% (vol/vol) formaldehyde were processed for paraffin sectioning and staining. For electron microscopy, embryonic hearts were fixed with 2.5% (vol/vol) glutaraldehyde in 0.1 M sodium phosphate (pH 7.4) for 1 hr at 4°C and immersed in 0.1 M sodium phosphate containing 7% (wt/vol) sucrose.

Cardiomyocyte Culture. Cells were prepared from 16.5-day-postcoitum (dpc) embryonic hearts of the ICR strain (17) and seeded at a density of 1×10^4 cells per 0.1 ml per well. After 2 days in culture in the presence of various factors, cells were pulse-labeled with [^{3}H]thymidine (0.5 μCi per well; 1 Ci = 37 GBq) for 12 hr and incorporated radioactivity was measured (18).

Colony-Forming Units in Spleen (CFU-S) Assays. Mononuclear cells (MNCs) were obtained from 13.5-dpc fetal livers, stained with Türk solution, and counted. Cells (2×10^5 cells) were intravenously injected into lethally irradiated C57BL/6 recipient mice (8 week old). Eleven days later, spleens were fixed with Bouin's solution and macroscopically observed colonies were counted. The CFU-S per fetal liver were then calculated based on the total number of MNCs in the donor liver.

Semisolid Colony-Forming Assays. MNCs from the 13.5-dpc fetal liver were suspended in minimum essential medium, α modification (1×10^5 cells per ml), containing 1.2% (wt/vol) methylcellulose, 1% bovine serum albumin, 100 μM 2-mercaptoethanol, and growth factors [murine interleukin 3 (500 units/ml)/human IL-6 (100 ng/ml)/human granulocyte colony-stimulating factor (10 ng/ml)/murine stem cell factor (100 ng/ml)/human erythropoietin (2 units/ml)]. Cells were divided in triplicate in 35-mm dishes (1 ml per dish) at 37°C for 14 days. Individual colonies were scored by morphology.

Flow Cytometry. After washing twice in PBS containing 3% (vol/vol) fetal calf serum and 0.05% sodium azide, thymocytes (1×10^5) were incubated for 20 min on ice with phycoerythrin- or fluorescein isothiocyanate-conjugated monoclonal antibodies and analyzed by FACScan (Becton Dickinson). Dead cells and nonlymphoid cells were excluded by gating for forward and side scatters. The monoclonal antibodies [30-H12 (Thy1.2), and RM2-5 (CD2)] were used according to the supplier's (PharMingen) procedures.

RESULTS

Targeted Disruption of the gp130 Gene Leads to Embryonic Lethality. The gene targeting was done as described in *Materials and Methods* (Fig. 1) and the targeted ES clones were injected into C57BL/6 blastocysts and obtained chimeric mice were crossed with normal C57BL/6 mice. Three lines of mice from independent ES cell clones transmitted the mutation through the germ line. Heterozygous mutant (gp130$^{+/-}$) mice did not show any apparent phenotype (data not shown). Out of 203 offspring from the heterozygous matings, no gp130$^{-/-}$ mice were observed when genotyped at 4–6 weeks of age, but gp130$^{+/-}$ mice appeared at a frequency of 64% (129 mice), which is close to the theoretical value, 67%, based on Mendelian laws. This indicated the lethal phenotype of the null mutation. To determine the time of death, embryos *in utero* and newborns derived from the gp130$^{+/-}$ intercrosses were analyzed for their gp130 genotype. As summarized in Table 1, gp130$^{-/-}$ embryos on 11.5 dpc were found at a frequency that roughly meets the Mendelian distribution. Thereafter recovery of live gp130$^{-/-}$ embryos decreased. Accordingly, in stages later than 12.5 dpc, gp130$^{-/-}$ embryos that were already dead upon inspection became apparent. At 18.5 dpc, live gp130$^{-/-}$ embryos were observed at a frequency of only 2.7% of the total live embryos, and eventually, no live gp130$^{-/-}$ newborns were found. Among the live gp130$^{-/-}$ embryos in particular after 13.5 dpc, ≈50% were smaller in size (mostly by ≈10%; in a few severe cases by up to 20%) than their gp130$^{+/+}$ and gp130$^{+/-}$ littermates. gp130$^{-/-}$ embryos displayed no obvious malformations in surface appearance at any stage examined. No significant phenotypic difference was observed among the three independent ES-clone-derived lines. Disappearance of the gp130 protein in the live mutant embryos was confirmed by immunoprecipitation followed by immunoblot analysis using antibodies to this protein (data not shown).

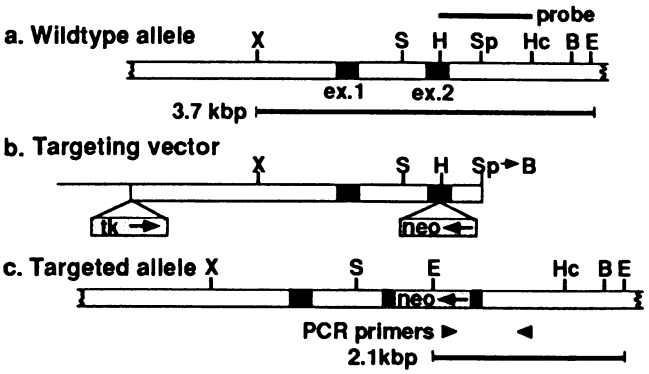

FIG. 1. Disruption of the gp130 gene. (*a*) The wild-type gp130 gene. Exons are indicated as solid boxes. (*b*) Targeting vector. Arrows indicate the transcriptional directions. (*c*) The mutated gp130 locus after homologous recombination. The Southern blot probe and PCR primers are indicated in *a* and *c*, respectively. The probe detects in the *Xho* I–*Eco*RI digests a 3.7-kbp or 2.1-kbp fragment in the wild-type or mutated allele, respectively. B, *Bam*HI; E, *Eco*RI; H, *Hin*dIII; Hc, *Hin*cII; S, *Sal* I; Sp, *Spe* I; X, *Xho* I.

Heart Abnormality in the gp130$^{-/-}$ Embryos. As shown in Fig. 2 *a–d*, the ventricular walls of the gp130$^{-/-}$ heart at 16.5 dpc were abnormally thin, showing a minimum thickness of one cell layer. This type of extreme abnormality in the myocardium was observed in all the 16.5 dpc (n = 5) and 17.5 dpc (n = 1) gp130$^{-/-}$ embryos examined histologically. In addition, gp130$^{-/-}$ heart was somewhat swollen and displayed a globular appearance with a round apex, probably due to the thinner ventricular walls. Despite the fact that a compact layer of the ventricle was extremely thin, trabeculation inside the ventricle chamber occurred normally in the gp130$^{-/-}$ hearts. In all six gp130$^{-/-}$ cases above at 16.5 dpc and 17.5 dpc, no ventricular septal defect was detected by examination of serial sections encompassing the entire ventricle. The ventricules of the gp130$^{-/-}$ embryos were indistinguishable from littermates' at 14.5 dpc (data not shown). Among the four histologically examined 15.5-dpc gp130$^{-/-}$ embryos, no extremely thin ventricular walls were detected. In two such cases, however, slightly hypoplastic development (≈30% reduction in the wall thickness at the site where the thinning was most obvious)

Table 1. Genotype of embryos after gp130$^{+/-}$ intercrosses

Age, dpc	Litters, no.	gp130 genotype, no. +/+	+/−	−/−	%
11.5	15	29 (2)	52 (2)	25 (4)	23.6
12.5	31	59	120 (4)	30 (8)	14.6
13.5	37	74	150 (2)	30 (26)	11.8
14.5	35	61	122 (2)	28 (20)	13.3
15.5	18	40	63 (3)	9 (8)	8.0
16.5	33	55	118 (3)	19 (8)	9.9
17.5	26	47	86 (1)	7 (9)	5.0
18.5	22	38	71 (1)	3 (7)	2.7
Newborns	6	17	34	0	

The number of dead embryos is given in parentheses. %, Percentage of live gp130$^{-/-}$ embryos.

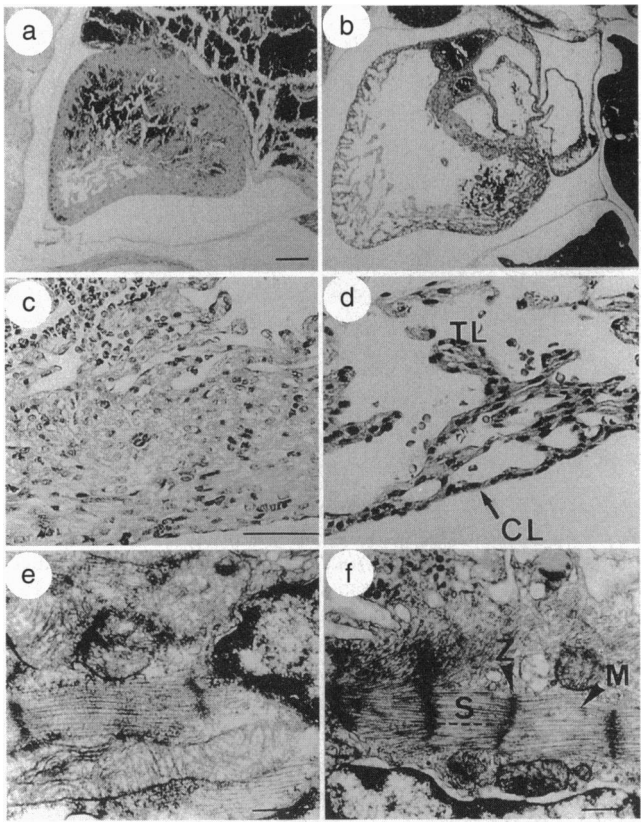

FIG. 2. Histological analysis of the control and gp130 null mutant embryonic hearts. (*a–d*) Sagittal sections of the right ventricle of control (*a* and *c*) and gp130$^{-/-}$ (*b* and *d*) 16.5-dpc littermates were stained by hematoxylin and eosin. (Bars: *a* and *b*, 200 μm; *c* and *d*, 50 μm, higher magnification views of the ventricular wall in *a* and *b*, respectively.) (*e* and *f*) Electron microscopic analysis of the 17.5-dpc compact layer of the embryonic heart from control (*e*) and gp130$^{-/-}$ littermate (*f*). M, myofibrils; S, sarcomere; Z, Z line. (Bars = 0.5 μm.)

of the ventricular myocardium was observed. Histologies of the remaining two gp130$^{-/-}$ hearts appeared normal and indistinguishable from those of gp130$^{+/+}$ and gp130$^{+/-}$ littermates throughout the sections.

To examine whether the subcellular ultrastructures of heart muscle cells were affected in gp130$^{-/-}$ embryos, electron microscopic examination was carried out. At 17.5 dpc, when the extreme thinning of the compact layer in the gp130$^{-/-}$ heart was observed, the presence and shape of subcellular structures such as nuclei, mitochondria, myofibrils, sarcomeric Z bands, and intercalated discs in the gp130$^{-/-}$ compact layer cells were of mature phenotype and indistinguishable from those of the control (Fig. 2 *e* and *f*). During normal mice embryogenesis, it has been reported that the compact layer cells at 14.5 dpc are not matured, having poorly organized myofibrils, but they become matured at 16.5 dpc showing well-organized myofibrils with clear Z bands (19). We considered that if premature differentiation of the compact layer cells occurred at, e.g., ≈14.5 dpc in the gp130$^{-/-}$ heart, this could lead to abolishment of the proliferation and/or maintenance of normal compact layer cells. By electron microscopic examination, we found the scarce appearance of organized myofibrils in the compact layer cells in hearts from both gp130$^{-/-}$ and control littermates at 14.5 dpc, indicating no sign of premature differentiation by the lack of gp130. Our data thus indicate that the extremely thin ventricular walls in the gp130$^{-/-}$ heart may not be due to a maturational alteration in cardiomyocytes.

We then examined whether the hypoplastic development of myocardium in the gp130$^{-/-}$ heart was due to the lack of

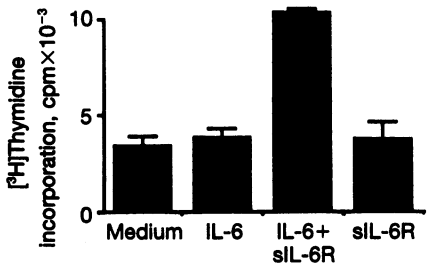

FIG. 3. Growth response of embryonic cardiomyocytes. Cardiomyocytes from 16.5-dpc ICR were cultured in the presence of the factors indicated in the figure and pulse-labeled with [^{3}H]thymidine. Data represent the incorporated radioactivities (averages of the triplicates) with SD (vertical bars).

proliferative signals transmitted from gp130 in cardiomyocytes. Since a combination of IL-6 and an extracellular soluble form of the IL-6R (sIL-6R) is known to interact with gp130 and induce its homodimerization to trigger cytoplasmic signaling (4), this combination was added to the cultured cardiomyocytes derived from 16.5-dpc normal ICR embryos. As shown in Fig. 3, stimulation of gp130 by the IL-6–sIL-6R complex led to an ≈2.5-fold increase in DNA synthesis in comparison with the medium control. Neither IL-6 nor sIL-6R alone showed any effect.

Hematopoietic Abnormality in gp130$^{-/-}$ Embryos. As shown in Fig. 4, the number of MNCs and CFU-S per liver at 13.5 dpc was dramatically reduced in the gp130$^{-/-}$ embryos. These values in the gp130$^{+/-}$ livers were intermediate between those in the gp130$^{+/+}$ and gp130$^{-/-}$ livers. The results indicated that gp130 plays a critical role in the development of the pluripotent stem cell pool in the fetal liver. Erythroid progenitors (erythroid burst-forming units, BFU-E) and granulocyte/macrophage progenitors (granulocyte/macrophage colony-forming units, CFU-GM) in the 13.5-dpc liver were then measured in semisolid cultures. These types of committed progenitors were also reduced.

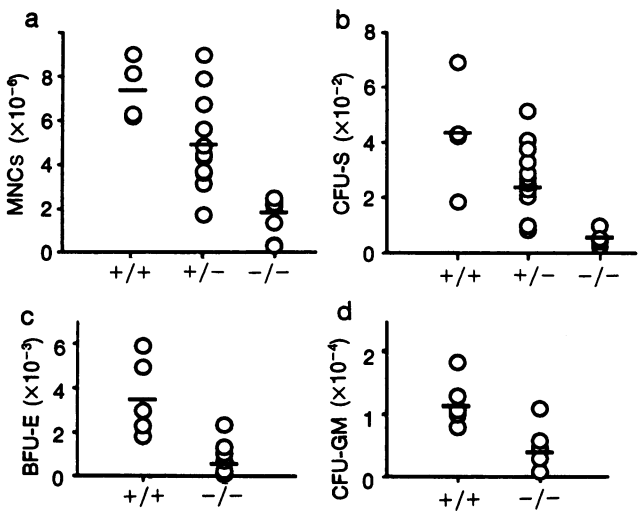

FIG. 4. Reduction of pluripotential and committed hematopoietic progenitors in 13.5-dpc gp130 null mutant fetal livers. (*a*) The number of MNCs in the liver from gp130$^{+/+}$ (n = 4), gp130$^{+/-}$ (n = 16), and gp130$^{-/-}$ (n = 7) embryos were analyzed. (*b*) CFU-S in the gp130$^{+/+}$ (n = 4), gp130$^{+/-}$ (n = 18), and gp130$^{-/-}$ (n = 4) fetal livers. (*c*) BFU-E in the gp130$^{+/+}$ (n = 5) and gp130$^{-/-}$ (n = 6) fetal livers. (*d*) CFU-GM in the gp130$^{+/+}$ (n = 6) and gp130$^{-/-}$ (n = 5) fetal livers. In all these assays, each dot represents the value derived from an individual fetal liver, and horizontal lines represent the mean of each group.

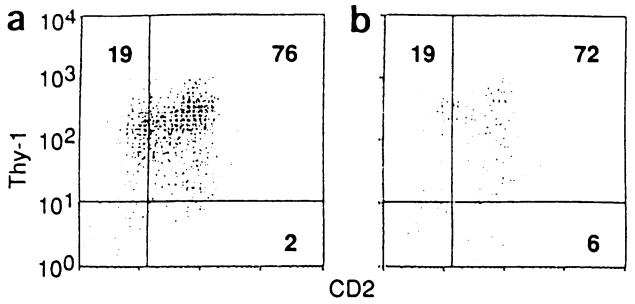

FIG. 5. Flow cytometric analysis of thymocytes in the 16.5-dpc gp130$^{-/-}$ fetal thymus. Analysis of thymocytes from control (*a*) and gp130$^{-/-}$ littermate (*b*) stained with a combination of phycoerythrin-coupled Thy-1 and fluorescein-isothiocyanate-coupled CD2 antibodies. Because of the extremely small number of thymocytes in the gp130$^{-/-}$ thymus, the total number of gated, analyzed, and displayed cells in *b* did not reach that in *a*. The percentage of cells with a particular cell surface expression phenotype is indicated within the appropriate quadrant.

As for a lymphoid tissue, the thymus was readily visible in 16.5-dpc gp130$^{-/-}$ embryos, although its size was smaller (≈50% that of the gp130$^{+/+}$ thymus). Thymocytes from 16.5-dpc gp130$^{+/+}$ or gp130$^{-/-}$ embryos were analyzed by flow cytometry for the expression of Thy1 and CD2. As shown in Fig. 5, the staining profile was similar in gp130$^{+/+}$ and gp130$^{-/-}$ embryos, although the absolute number of thymocytes was considerably smaller in the latter. It is thus indicated that although T-lineage cells emerged, their number was severely reduced by the lack of gp130, probably due to the extremely reduced stem cell pool.

Although BFU-E numbers were reduced in the gp130$^{-/-}$ fetal livers, most of the gp130$^{-/-}$ fetuses did not appear significantly anemic. However, ≈20% of gp130$^{-/-}$ embryos at 15.5–18.5 dpc exhibited paleness. In these anemic gp130$^{-/-}$ embryos, there were no signs of hemorrhage. Peripherally existing red blood cells in the blood vessels of the pale 16.5-dpc embryos were inspected as shown in Fig. 6. A larger number of nucleated erythrocytes (and thus a smaller number of enucleated erythrocytes) were found in the blood vessels of the gp130$^{-/-}$ embryo than in the gp130$^{+/+}$ littermate.

DISCUSSION

One of the most striking observations in the gp130 knockout mice is the extreme hypoplastic development of ventricular myocardium. In these mice, ventricular myocardium developed normally until 14.5 dpc, but from 16.5 dpc on, its extreme thinning became apparent without accompanying septal and trabecular defect. Developmental cardiac abnormalities have also been observed in mice disrupted for some other genes. Mice homozygous for a retinoid X receptor α mutation were nonviable and exhibited considerably thinner compact layer of the ventricular walls (20, 21). However, this abnormality was apparent as early as 13.5 dpc and accompanied by ventricular septal defect. Furthermore, precocious differentiation of the subepicardial myocytes in these mice was obvious at 14.5 dpc, and the ultrastructures of such cells were already of mature type at this stage (21). A homozygous mutation in the transcriptional enhancer factor 1 (TEF-1) gene also led to the abnormal thin ventricular walls, but this phenotype was apparent even earlier (at 11.5 and 12.5 dpc) and accompanied by poor trabeculation, unlike in the case of gp130 or retinoid X receptor α deficiency (22). The right ventricle of platelet-derived growth factor B-deficient embryos was, again, abnormally thin-walled, but this was observed on 17.5 and 18.5 dpc (23). Considering the variety of phenotypes described above,

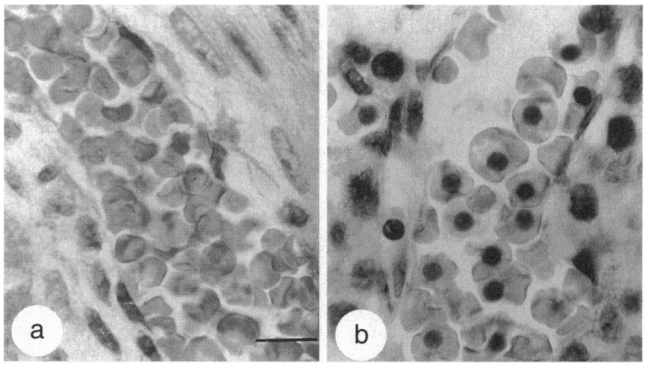

FIG. 6. Erythroid lineage cell abnormality in the 16.5-dpc gp130 null mutant. Red blood cells in the sections of control (*a*) and gp130$^{-/-}$ (*b*) peripheral blood vessels were stained with hematoxylin and eosin. (Bars = 10 μm.)

each of these mutations presumably affects heart development at different time points in a different manner.

The number of cardiomyocytes in the thin-walled compact layer of the gp130$^{-/-}$ ventricle was very much reduced at 16.5 dpc and later. These cells, however, possessed normal ultrastructural components. They normally expressed cardiomyocyte-specific markers as did gp130$^{+/+}$ cardiomyocytes. The myosin light chain *1v* and *2v* genes as well as the atrial natriuretic peptide gene (24) were normally expressed in both 14.5- and 17.5-dpc gp130$^{-/-}$ cardiomyocytes as examined by PCR analysis (data not shown). Thus, with the result that stimulation of gp130 by the IL-6–sIL-6R complex induced DNA synthesis in 16.5-dpc cardiomyocytes, it is suggested that while gp130 signaling may play a role in the growth of these cells, it may not influence their differentiation, at least at stages around 14.5–16.5 dpc. Our findings suggest possible existence of a gp130-stimulatory cytokine that regulates heart muscle cell growth. A cytokine called CT-1 has recently been cloned that acts on neonatal cardiomyocytes to cause hypertrophy and whose structure is closely related to, e.g., LIF and CNTF (25). CT-1 is suggested to act through the LIF receptor–gp130 heterodimer, since CT-1 and LIF cross-compete for binding to their target cells and CT-1 binding to these cells can be inhibited by anti-gp130 antibody (3). A role of gp130 in the cardiomyocyte regulation has also been shown by transgenic mice that overexpress both IL-6 and IL-6R; they exhibit pathological ventricular hypertrophic change in adulthood (17). Because the size of each cardiomyocyte in the gp130$^{-/-}$ embryonic heart appeared to be comparable to that observed in the gp130$^{+/+}$ heart, the function of CT-1, assuming it to be mediated during embryogenesis by gp130, might be to induce proliferation rather than hypertrophy. An alternative possible stimulator of gp130 in embryonic heart muscle cells is the complex of IL-6 and sIL-6R, which exists physiologically (26). Furthermore, serum sIL-6R level increases in accordance with progression of gestational stages (27).

Since ≈20% of the gp130$^{-/-}$ embryos were anemic at 15.5–18.5 dpc, one could argue that poor oxygenation might have led to the hypoplastic development of myocardium in these embryos. However, considering that 100% of the gp130$^{-/-}$ embryos showed heart abnormalities at 16.5 dpc, this argument does not appear to be true. Furthermore, most of the mutant mice showing severe anemia during embryogenesis [dominant white spotting (*W*), steel (*sl*), and *PU-1* mutant mice] do not reportedly exhibit the extreme thinning of the ventricular walls (28, 29).

The lack of gp130 decreased the number of pluripotential hematopoietic stem cells (by 88% based on the average CFU-S values in Fig. 4*b*) and committed hematopoietic progenitors (by 86% for BFU-E and by 66% for CFU-GM as calculated from Fig. 4 *c* and *d*). The decrease in the committed progen-

itors might be due to the greatly reduced number of pluripotential ones. In addition to the decrease in T-lineage cells (Fig. 5), the megakaryocyte number appeared to be reduced. Megakaryocytes were detectable in fetal liver sections from 16.5-dpc gp130$^{-/-}$ and gp130$^{+/+}$ littermates at a roughly comparable frequency (data not shown). Considering the smaller size of the gp130$^{-/-}$ fetal liver, the total number of megakaryocytes per liver in this genotype was reduced. Thus, the extreme reduction in pluripotential hematopoietic stem cell pools by the lack of gp130 may have led to a similar decrease in the committed progenitors and differentiated cells. Although few in numbers, some pluripotent hematopoietic progenitors did emerge in the absence of gp130 signaling, and once emerged, they appeared to remain multipotent and capable of differentiating into at least the lineages mentioned above. In this relation, it should be noted that colonizing efficiency of gp130$^{-/-}$ hematopoietic progenitors in the recipient spleen was not much impaired by the lack of gp130: The average colony number in the spleen of a recipient mouse inoculated with 2×10^5 gp130$^{-/-}$ fetal liver-derived MNCs was 6.2 ± 2.9 for gp130$^{-/-}$ ($n = 4$) and 8.7 ± 3.0 for gp130$^{+/+}$ ($n = 4$).

There were variations in the numbers of liver MNCs and CFU-S among individual fetuses of the same genotype (see Fig. 4 *a* and *b*). In addition, among the gp130$^{-/-}$ embryos, the severity of anemic paleness varied considerably (only 20% showed significant anemia). One explanation for these fluctuations might be that the genetic background of the embryos was not uniform, but rather a mixture of 129 and C57BL/6.

The observation that hematopoietic stem cells are reduced in gp130$^{-/-}$ embryos suggests that gp130 signaling plays an important role in the self-renewal processes of the stem cells. In this relation, it is important to note that a complex of IL-6 and sIL-6R acted synergistically with stem cell factor in the *ex vivo* expansion of primitive hematopoietic progenitor cells from human cord blood (30). Mutations at the *W* locus in mouse severely affect the development of hematopoietic precursors for multiple lineages. This may raise a possibility that the signals through c-Kit and gp130 may cooperate in the self-renewal process. gp130 and c-Kit signals also synergized in the proliferation and terminal maturation of human erythroid lineage cells (X. Sui, K. Tsuji, S. Tajima, R. Tanaka, K. Muraoka, Y. Ebihara, K. Ikebuchi, K. Yasukawa, T.T., T.K., and T.N., unpublished data), which is reminiscent of the anemia observed in some of the gp130$^{-/-}$ embryos.

In conclusion, the gp130 deficiency was lethal and affected to a great extent ventricular myocardial development and hematopoiesis. The rest of organs are being examined in detail. Since gp130 is expressed in every organ, it could be possible that even the apparently normally developed organs in the gp130$^{-/-}$ fetuses would exhibit abnormalities if the fetuses were to continue to develop by rescuing such a defect as in the heart. Tissue-specific targeting of the gp130 gene, for instance in the nervous system, would clarify the role of gp130 in various organs in more detail.

We thank Ms. K. Kubota for her excellent secretarial assistance and Drs. K. Fujiwara and T. Ishibashi for helpful comments. We also thank Dr. M. Lamphier for a critical review of the manuscript. This study was supported by grants from the Ministry of Education, Science and Culture, the Ministry of Health and Welfare, the Uehara Memorial Foundation, the Naito Foundation, and the Kowa Life Science Foundation.

1. Kishimoto, T., Taga, T. & Akira, S. (1994) *Cell* **76,** 253–262.
2. Taga, T., Hibi, M., Hirata, Y., Yamasaki, K., Yasukawa, K., Matsuda, T., Hirano, T. & Kishimoto, T. (1989) *Cell* **58,** 573–581.
3. Pennica, D., Shaw, K. J., Swanson, T. A., Moore, M. W., Sheliton, D. L., Zioncheck, K. A., Rosenthal, A., Taga, T., Paoni, N. F. & Wood, W. I. (1995) *J. Biol. Chem.* **270,** 10915–10922.
4. Murakami, M., Hibi, M., Nakagawa, M., Nakagawa, T., Yasukawa, K., Yamanishi, K., Taga, T. & Kishimoto, T. (1993) *Science* **260,** 1808–1810.
5. Davis, S., Aldrich, T. H., Stahl, N., Pan, L., Taga, T., Kishimoto, T., Ip, N. Y. & Yancopoulos, G. D. (1993) *Science* **260,** 1805–1808.
6. Narazaki, M., Witthuhn, B. A., Yoshida, K., Silvennoinen, O., Yasukawa, K., Ihle, J. N., Kishimoto, T. & Taga, T. (1994) *Proc. Natl. Acad. Sci. USA* **91,** 2285–2289.
7. Stahl, N., Boulton, T. G., Farruggella, T., Ip, N. Y., Davis, S., Witthuhn, B. A., Quelle, F. W., Silvennoinen, O., Barbieri, G., Pellegrini, S., Ihle, J. N. & Yancopoulos, G. D. (1994) *Science* **263,** 92–95.
8. Stahl, N., Farruggella, J., Boulton, T. G., Zhong, Z., Darnel, J. E. & Yancopoulos, G. D. (1995) *Science* **267,** 1349–1353.
9. Akira, S., Nishio, Y., Inoue, M., Wang, X.-J., Wei, S., Matsusaka, T., Yoshida, K., Sudo, T., Naruto, M. & Kishimoto, T. (1994) *Cell* **77,** 63–71.
10. Lütticken, C., Wegenka, U. M., Yuan, J., Buschmann, J., Schindler, C., Ziemiecki, A., Harpur, A. G., Wilks, A. F., Yasukawa, K., Taga, T., Kishimoto, T., Barbieri, G., Pellegrini, S., Sendtner, M., Heinrich, P. C. & Horn, F. (1994) *Science* **263,** 89–92.
11. Nakajima, T., Kinoshita, S., Sasagawa, T., Sasaki, K., Naruto, M., Kishimoto, T. & Akira, S. (1993) *Proc. Natl. Acad. Sci. USA* **90,** 2207–2211.
12. Saito, M., Yoshida, K., Hibi, M., Taga, T. & Kishimoto, T. (1992) *J. Immunol.* **148,** 4066–4071.
13. Stewart, C. L., Kaspar, P., Brunet, L. J., Bhatt, H., Gadi, I., Köntgen, F. & Abbondanzo, J. S. (1992) *Nature (London)* **359,** 76–79.
14. Masu, Y., Wolf, E., Holtmann, B., Sendtner, M., Brem, G. & Thoenen, H. (1993) *Nature (London)* **365,** 27–32.
15. Kopf, M., Baumann, H., Freer, G., Freudenberg, M., Lamers, M., Kishimoto, T., Zinkernagel, R., Bluethmann, H. & Köhler, G. (1994) *Nature (London)* **368,** 339–342.
16. Mansour, S. L., Thomas, K. R. & Capecchi, M. R. (1988) *Nature (London)* **336,** 348–352.
17. Hirota, H., Yoshida, K., Kishimoto, T. & Taga, T. (1995) *Proc. Natl. Acad. Sci. USA* **92,** 4862–4866.
18. Yoshida, K., Chambers, I., Nichols, J., Smith, A. G., Saito, M., Yasukawa, K., Shoyab, M., Taga, T. & Kishimoto, T. (1994) *Mech. Dev.* **45,** 163–171.
19. Rumyantsev, P. P. (1977) *Int. Rev. Cytol.* **91,** 187–273.
20. Sucov, H. M., Dyson, E., Gumeringer, C. L., Price, J., Chien, K. R. & Evans, R. M. (1994) *Genes Dev.* **8,** 1007–1018.
21. Kastner, P., Grondona, J. M., Mark, M., Gansmuller, A., Lemeur, M., Decimo, D., Vonesch, J. L., Dollé, P. & Chambon, P. (1994) *Cell* **78,** 987–1003.
22. Chen, Z., Friedrich, G. A. & Soriano, P. (1994) *Genes Dev.* **8,** 2293–2301.
23. Levéen, P., Peckny, M., Gebre-Medhin, S., Swolin, B., Larsson, E. & Betsholtz, C. (1994) *Genes Dev.* **8,** 1875–1887.
24. Chien, K. R., Zhu, H., Knowlton, K. U., Miller-Hans, W., van Wilson, M., O'Brien, T. X. & Evans, S. M. (1993) *Annu. Rev. Physiol.* **55,** 77–95.
25. Pennica, D., King, K., Shaw, K. J., Luis, E., Rullamas, J., Luoh, S.-M., Darbonne, W. C., Knutzon, D. S., Yen, R., Chien, K. R., Baker, J. B. & Wood, W. (1995) *Proc. Natl. Acad. Sci. USA* **92,** 1142–1146.
26. Suzuki, H., Yasukawa, K., Saito, T., Narazaki, M., Hasegawa, A., Taga, T. & Kishimoto, T. (1993) *Eur. J. Immunol.* **23,** 1078–1082.
27. Maeda, T. M., Yamaguchi, M., Taga, T., Kishimoto, T., Wada, K., Ikegami, H., Kurachi, H. & Miyake, A. (1994) *Biochem. Biophys. Res. Commun.* **205,** 998–1003.
28. Russell, E. S. (1979) *Adv. Genet.* **20,** 357–460.
29. Scott, E. W., Simon, M. C., Anastasi, J. & Singh, H. (1994) *Science* **265,** 1573–1577.
30. Sui, X., Tsuji, K., Tanaka, R., Tajima, S., Muraoka, K., Ebihara, Y., Ikebuchi, K., Yasukawa, K., Taga, T., Kishimoto, T. & Nakahata, T. (1995) *Proc. Natl. Acad. Sci. USA* **92,** 2859–2863.